



Contents lists available at ScienceDirect

# Atmospheric Environment

journal homepage: [www.elsevier.com/locate/atmosenv](http://www.elsevier.com/locate/atmosenv)

Short communication

## Time effects of high particulate events on the critical conversion point of ground-level ozone



Norrimi Rosaida Awang<sup>b</sup>, Nor Azam Ramli<sup>a,\*</sup>, Syabiha Shith<sup>a</sup>, Noor Faizah Fitri Md Yusof<sup>a</sup>, Nazatul Syadia Zainordin<sup>c</sup>, Nurulilyana Sansuddin<sup>d</sup>, Nurul Adyani Ghazali<sup>e</sup>

<sup>a</sup> Environmental Assessment and Clean Air Research, School of Civil Engineering, Engineering Campus, Universiti Sains Malaysia, 14300, Nibong Tebal, Pulau Pinang, Malaysia

<sup>b</sup> Faculty of Earth Science, Universiti Malaysia Kelantan Kampus Jeli, Locked Bag No. 100, 17600, Jeli, Kelantan, Malaysia

<sup>c</sup> Department of Environmental Management, Faculty of Environmental Studies, Universiti Putra Malaysia, 43400 Serdang, Selangor, Malaysia

<sup>d</sup> School of Health Sciences, Health Campus, Universiti Sains Malaysia, 16150 Kubang Kerian, Kelantan, Malaysia

<sup>e</sup> School of Marine Engineering, Universiti Malaysia Terengganu, 21030 Kuala Terengganu, Terengganu, Malaysia

### ARTICLE INFO

#### Keywords:

Ozone production  
Anthropogenic sources  
Ozone precursor  
Photochemical reaction  
Particulate matter

### ABSTRACT

Particulate matter (PM), especially those with an aerodynamic particle size of less than 10  $\mu\text{m}$  ( $\text{PM}_{10}$ ), is typically emitted from transboundary forest fires. A large-scale forest fire may contribute to a haze condition known as a high particulate event (HPE), which has affected Southeast Asia, particularly Peninsular Malaysia, for a long time. Such event can alter the photochemical reactions of secondary pollutants. This work investigates the influence of PM on ground-level ozone ( $\text{O}_3$ ) formation during HPE. Five continuous air quality monitoring stations from different site categories (i.e., industrial, urban and background) located across Peninsular Malaysia were selected in this study during the HPEs in 2013 and 2014. Result clearly indicated that  $\text{O}_3$  concentrations were significantly higher during HPE than during non-HPE in all the sites. The  $\text{O}_3$  diurnal variation in each site exhibited a similar pattern, whereas the magnitudes of variation during HPE and non-HPE differed. Light scattering and atmospheric attenuation were proven to be associated with HPE, which possibly affected  $\text{O}_3$  photochemical reactions during HPE. Critical conversion time was used as the main determining factor when comparing HPE and non-HPE conditions. A possible screening effect that resulted in the shifting of the critical transformation point caused a delay of approximately of 15–30 min. The shifting was possibly influenced by the attenuation of sunlight in the morning during HPE. A negative correlation between  $\text{O}_3$  and  $\text{PM}_{10}$  was observed during the HPE in Klang in 2013 and 2014, with  $-0.87$ . Essentially, HPE with a high PM concentration altered ground-level  $\text{O}_3$  formation.

### 1. Introduction

Atmospheric haze is typically associated with reduced visibility due to an increase in aerosol loading, which can substantially impact the radiative balance of the direct reflection of the Earth (or indirect reflection due to cloud formation) and the absorption of incoming solar radiation (Seinfeld and Pandis, 2006). In Southeast Asia, atmospheric haze, which is commonly known as smoke haze due to its large-scale plumes or airborne pollutants, is associated with wildfires or biomass burning resulting from the open burning of agricultural residues, slash-and-burn practices, and forest fires (Velasco and Rastan, 2015; Ahmed et al., 2016). In addition to biomass burning, atmospheric haze episodes have also been attributed to anthropogenic sources, which are mainly contributed by growing urbanisation and expanding economic

activities. In Malaysia, atmospheric haze is predominantly associated with surges in the concentration of ambient particulates (Rahman, 2013). Accordingly, the term ‘high particulate event (HPE)’ is used in the current study to refer to atmospheric haze episodes due to particulates.

The physical, chemical and optical properties of HPE can have physical, biological and economic effects on ecosystems, human health and water budget (Xu et al., 2015; Zhou et al., 2015). Severe and long-term HPE can indirectly affect the efficiency of vegetative photosynthesis (Xu et al., 2015) given that HPE can reduce atmospheric visibility by 20%–90% (Wang, 2003). The deposition of water-insoluble aerosols on plant leaves may reduce vegetative photosynthesis by up to 35% (Bergin et al., 2001), intensify crop yield and possibly increase the greenhouse effect. Scientific evidence has also shown a strong

\* Corresponding author.

E-mail address: [ceazam@usm.my](mailto:ceazam@usm.my) (N.A. Ramli).

association between HPE and certain health problems, such as premature mortality, cardiovascular and respiratory diseases and lung cancer (Olmo et al., 2011). The combination of prolonged dry weather in Southeast Asia and the widespread anthropogenic land-clearing fires in central Sumatera reduced visibility and air quality in Peninsular Malaysia, including Singapore, during an extensive and large-scale HPE in June 2013. During this event, more than 600 schools in southern Peninsular Malaysia were closed because the Air Pollution Index (API) exceeded the hazardous point of 300. At the peak of the event, two districts were placed under a state of emergency because the API reached 700 (DoE, 2013; Rahman, 2013).

The adverse impacts of the 2013 HPE on the air quality of countries along the Strait of Malacca (i.e. Malaysia, Singapore and Indonesia) have been reported in many studies in terms of primary observations during the event (Othman et al., 2014) and direct impacts on ecosystems, environmental outcomes and economic losses (Velasco and Rastan, 2015). In addition, several studies have investigated the characteristics and composition of particulates (Fujii et al., 2015; Zhou et al., 2015; Ahmed et al., 2016), the link between aerosol optical depth and free space optics (Maghami et al., 2015; Malik and Singh, 2015), transboundary smoke–haze dispersion (Reid et al., 2013) and numerical modelling (Reddington et al., 2014).

Ozone ( $O_3$ ) exists as a secondary pollutant in the lower atmosphere, where its formation and destruction highly depend on ultraviolet (UV) radiation and the intensity of its precursors, such as nitrogen oxides ( $NO_x$ ) (Ainsworth et al., 2012; Hassan et al., 2013; Alghamdi et al., 2014). Aside from being a secondary pollutant that requires UV light to complete its photochemical reactions,  $O_3$  is a noxious air pollutant and is recognised as the second most significant air pollutant in Malaysia (Rahman, 2013).  $O_3$  is toxic to humans and vegetation at the ground level due to its capability to oxidise biological tissues (Brimblecombe, 2009; Pugliese et al., 2014). The transformational characteristics of  $O_3$  during HPE are crucial for understanding the role of this air pollutant in such event. HPE conditions may trigger high  $O_3$  photochemical reactions, which intensify the impacts of HPE due to large increments of ambient particulates and  $O_3$ .

Studies on  $O_3$  formation and variation are regarded as complex because of various possible precursors, photochemical processes, sunlight intensities and meteorological factors (Chattopadhyay and Chattopadhyay, 2011; Toh et al., 2013). Different approaches, including direct observation (Azmi et al., 2010) and empirical modelling (Sousa et al., 2007; Ozbay et al., 2011; Dominick et al., 2012), have been utilised to explain these processes. Awang et al. (2015) introduced the use of critical transformational time (CCT), which is determined based on the photochemical reactions of  $O_3$  formation. CCT is obtained based on  $O_3$  critical transformational point (CCP), which is a point when the rate of nitrogen dioxide ( $NO_2$ ) photolysis is higher than that of nitric oxide (NO) titration, thereby resulting in the accumulation of  $O_3$  concentration.

The current study clearly indicates that CCT is crucial to daily  $O_3$  transformation, and this period can better represent  $O_3$  variations than daytime. Moreover, after analysing 12 years of  $O_3$  transformation and its precursor monitoring records, Awang et al. (2016) found that CCT in Malaysia typically occurs between 8 a.m. and 11 a.m. during non-HPE. However, the finding emphasised that several changes might have occurred during CCP time due to changes in atmospheric conditions, surges in precursors or obstructions of UV intensity. HPE can alter a single or a mixture of  $O_3$  photochemical ingredients; hence, understanding  $O_3$  CCP during HPE may provide crucial evidence for  $O_3$  transformational behaviour. Therefore, this study aims to further explore the possibilities of using CCP to explain  $O_3$  production during HPE and to establish a possible relationship between gases and particulate pollutants.

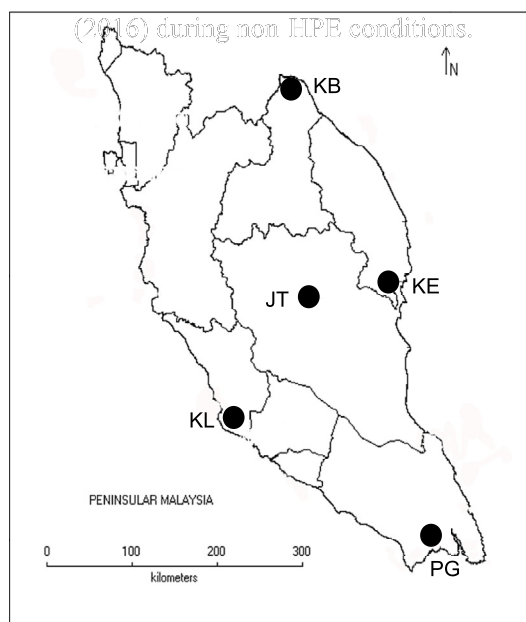


Fig. 1. Location of selected monitoring stations in Malaysia.

## 2. Methods

### 2.1. Location of sampling station

This study focused on the 2013 and 2014 HPEs. The duration of an HPE is determined based on API value because an HPE is considered to occur once the API value continuously exceeds 100 for 24 h. Five continuous air quality monitoring stations located across Peninsular Malaysia were selected in this study, as shown in Fig. 1. These stations were grouped into three categories, namely, industrial [Pasir Gudang (PG) and Kemaman (KE)], urban [Kota Bharu (KB) and Klang (KL)] and background [Jerantut (JT)], for HPE and non-HPE. The occurrence of an HPE for over 24 h was the main criterion for selecting the study areas, whereas the stations were chosen from among those included in Awang et al. (2016) to account for variations during non-HPE periods. The details of the occurrence period of HPE in 2013 and 2014 are provided in Table 1. The data collected was annual data in 2013 and 2014. Most of the selected HPE dates occurred in 2013, except for those in Klang, where the number of HPE hours was between 28 h and 112 h. Meanwhile, non-HPE data refer to the remaining data for that month of the year. All the selected stations are under a tropical climate characterised by a uniform high temperature ranging from 22 °C to 24 °C during nighttime and from 27 °C to 30 °C during daytime. The mean annual rainfall is 2670 mm (Ghazali et al., 2010; Md Yusof et al., 2010), and relative humidity ranges from 70% to 90%.

### 2.2. Data collection

The hourly secondary monitoring records of  $O_3$ , particulate matter (PM) with an aerodynamic diameter less than 10  $\mu m$  ( $PM_{10}$ ),  $NO$ ,  $NO_2$  concentrations and meteorological parameters (i.e. wind speed, WS; temperature, T and relative humidity, RH) were obtained from the Air Quality Division, Department of Environment (DoE), Malaysia. These variables were selected based on their relationship with  $O_3$  production (Clapp and Jenkin, 2001; Seinfeld and Pandis, 2006).

Hourly  $O_3$  concentration was monitored using the Model 400E UV Absorption Ozone Analyser (DoE, 2010). This analyser applies the Beer–Lambert law, which is based on the internal electronic resonance of  $O_3$  molecules with a UV light absorption of 254 nm in measuring low ranges of  $O_3$  concentration in ambient air (Ghazali et al., 2010; Mohammed et al., 2013). Changes in ambient  $NO_2$  and  $NO$

**Table 1**  
 Details of the occurrence periods of HPE and non-HPE in 2013 and 2014.

Month	Stations	Station ID	HPE Period				HPE Hour	Non-HPE Hour
			Start	Time	End	Time		
<b>2013</b>								
June	Pasir Gudang (I)	PG	21/6/13	7 a.m.	23/6/13	3 p.m.	56	664
	Kemaman (I)	KE	21/6/13	7 a.m.	24/6/13	3 a.m.	68	652
	Kota Bharu (U)	KB	24/6/13	1 a.m.	25/6/13	4 a.m.	28	692
	Klang (U)	KL	22/6/13	7 a.m.	26/6/13	2 p.m.	112	608
	Jerantut (B)	JT	24/6/13	1 a.m.	25/6/13	12 a.m.	47	673
<b>2014</b>								
March	Klang (U)	KL	15/3/14	3 a.m.	19/3/14	3 a.m.	97	647

\*Note: I-industrial; U-urban; B-background.

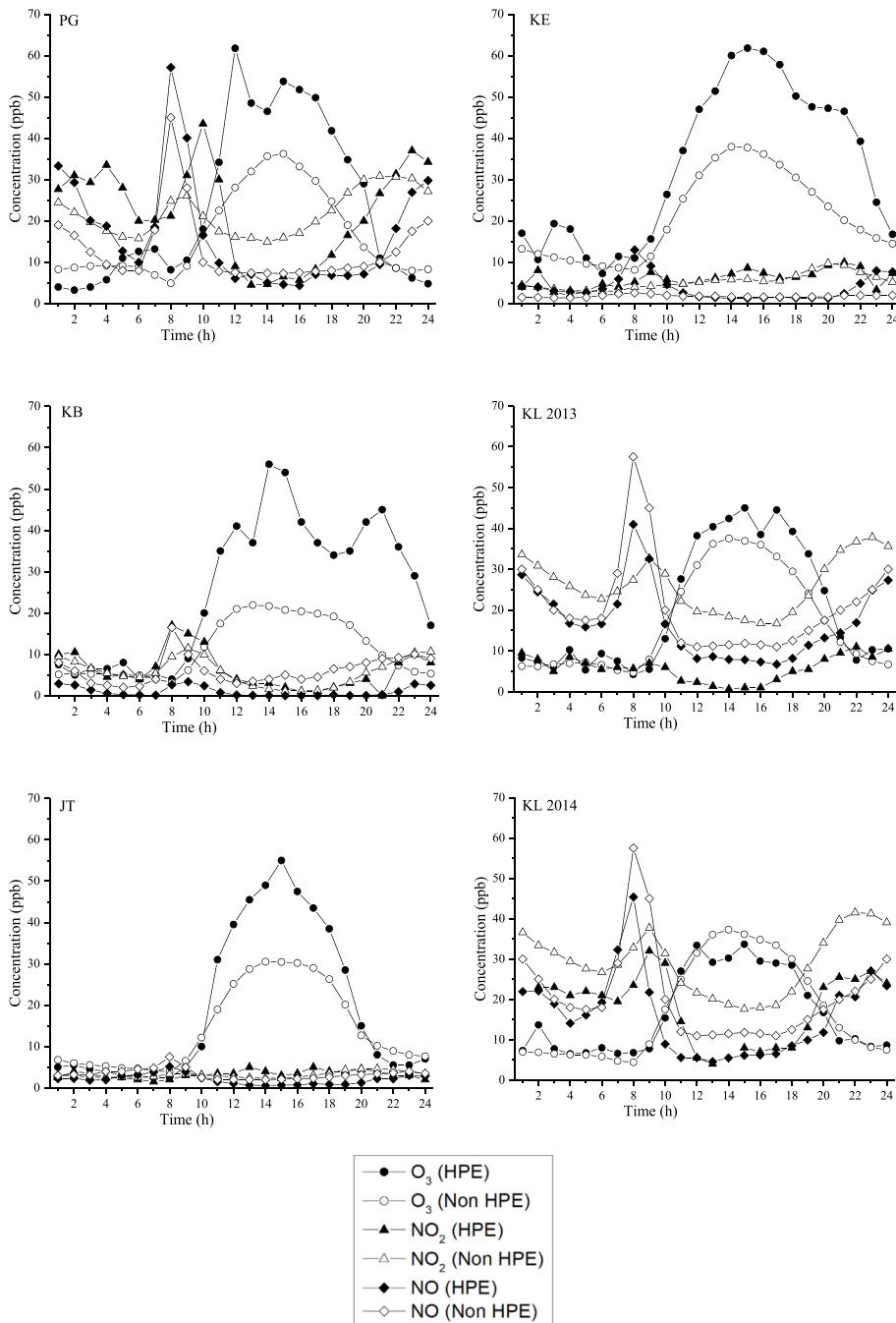


**Fig. 2.** CCP based on the intersection among O<sub>3</sub>, NO<sub>2</sub> and NO in a composite diurnal plot during HPE and non-HPE.

**Table 2**  
CCP time based on the composite diurnal plots for all the monitoring stations.

Station	Time of CCP (a.m.)	
	HPE	Non HPE
PG	10.50	10.30
KE	8.10	*NC
KB	9.30	9.45
KL (2013)	9.10	10.50
JT	8.20	8.40
KL (2014)	10.30	10.05

\*NC is no clear variations.

concentrations were collected using Model 200A NO/NO<sub>2</sub>/NO<sub>x</sub> Analyser (Ghazali et al., 2010; Latif et al., 2014). This analyser applies chemiluminescence detection principles to determine NO<sub>2</sub> and NO concentrations in ambient air; it has been proven to provide sensibility, stability and ease of use for continuous monitoring in ambient or diluted air (DoE, 2010). The Beta Attenuation Mass Monitor (BAM-1 020) was used to monitor ambient PM<sub>10</sub>. Meteorological parameters were monitored using Met One 062 sensor for temperature, Met One 083D sensor for relative humidity, Met One 010C sensor for wind speed and Met One 020C for wind direction (Latif et al., 2014).

The obtained secondary data were regularly subjected to standard quality control processes and quality assurance procedures (Mohammed et al., 2013). The procedures used for continuous monitoring are in accordance with the standard procedures outlined by internationally recognised environmental agencies, such as the United States Environmental Protection Agency (Latif et al., 2014).

### 2.3. Determination of CCP

In this study, the CCP of each station was determined using two techniques: composite diurnal plot and O<sub>3</sub> photochemistry rate. The

details of both techniques, particularly during non-HPE conditions, are discussed in Awang et al. (2015, 2016). Similar methods were used to determine CCP during HPE. The intersection among O<sub>3</sub>, NO<sub>2</sub> and NO in diurnal plots is known as the CCP point. If the exact intersection point cannot be determined, then the CCP point is obtained by estimating the interception point.

### 3. Results and discussions

The composite diurnal plots in all the selected stations during HPE and non-HPE in 2013 and 2014 are illustrated in Fig. 2. The result clearly indicated that O<sub>3</sub> concentrations were significantly higher during HPE than during non-HPE. The maximum diurnal O<sub>3</sub> concentrations during HPE for PG, KE, KB, JT, KL (2013) and KL (2014) were 61.75, 61.80, 65.00, 55.00, 45.00 and 33.67 ppb, respectively. O<sub>3</sub> concentration in all sites exhibit the same trend, during HPE was relatively higher than non-HPE in all sites, except for KL (2014). The concentrations of NO and NO<sub>2</sub> show a fluctuation in PG and KE where the concentrations during HPE was higher compared to non-HPE contrast with the diurnal trend observed in KB, JT, KL (2013), and KL (2014).

The results showed that the O<sub>3</sub> diurnal variation of each site exhibited a similar pattern, whereas the magnitudes of variations during HPE and non-HPE differed. The diurnal pattern of O<sub>3</sub> for each site is characterised by a maximum concentration in the afternoon and a minimum concentration during nighttime (Turias et al., 2008; Jones and Kirby, 2009) parallel to variations in solar radiation intensity during the day, which is a favourable condition for promoting photochemical reactions. In normal non-HPE days, solar radiation with a wavelength of less than 400 nm has sufficient energy to photolyse NO<sub>2</sub> into NO and oxygen atom (O) (Seinfeld and Pandis, 2006; Ghazali et al., 2010). This solar radiation was the same during HPE, but was affected by gases and particles in absorption and scattering process. This reaction is called NO<sub>2</sub> photolysis. It is regarded as the main reaction that

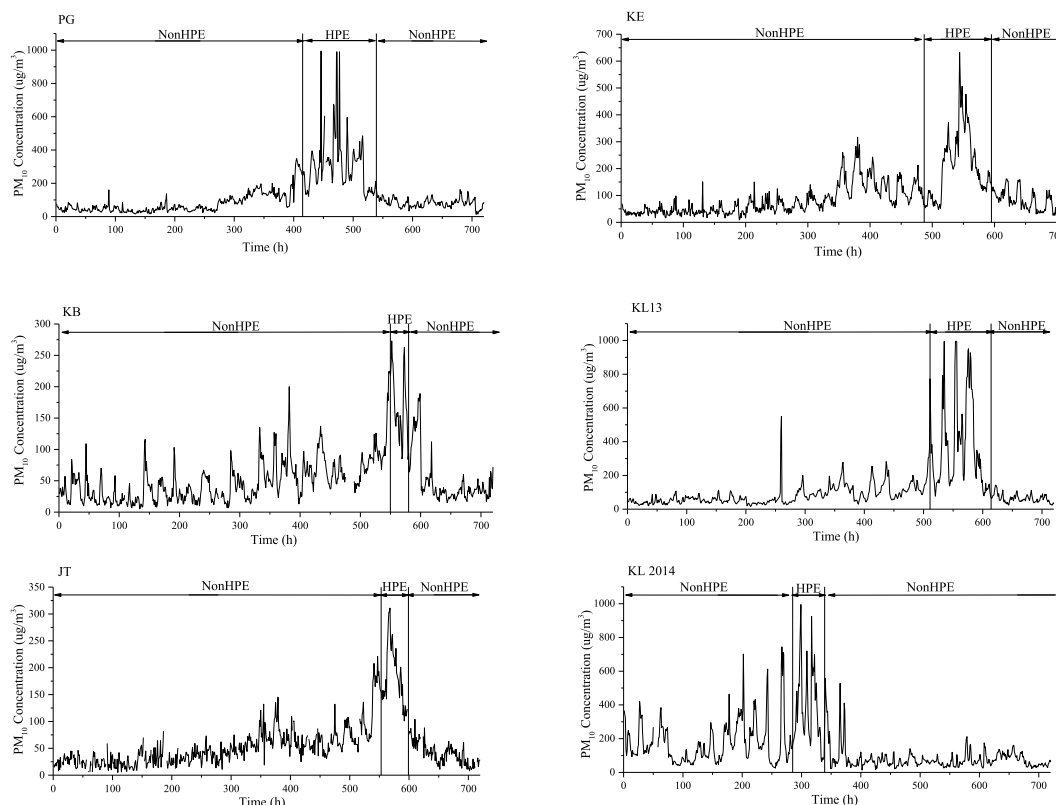


**Fig. 3.** Time-series plot of PM<sub>10</sub> concentrations during HPE and non-HPE.

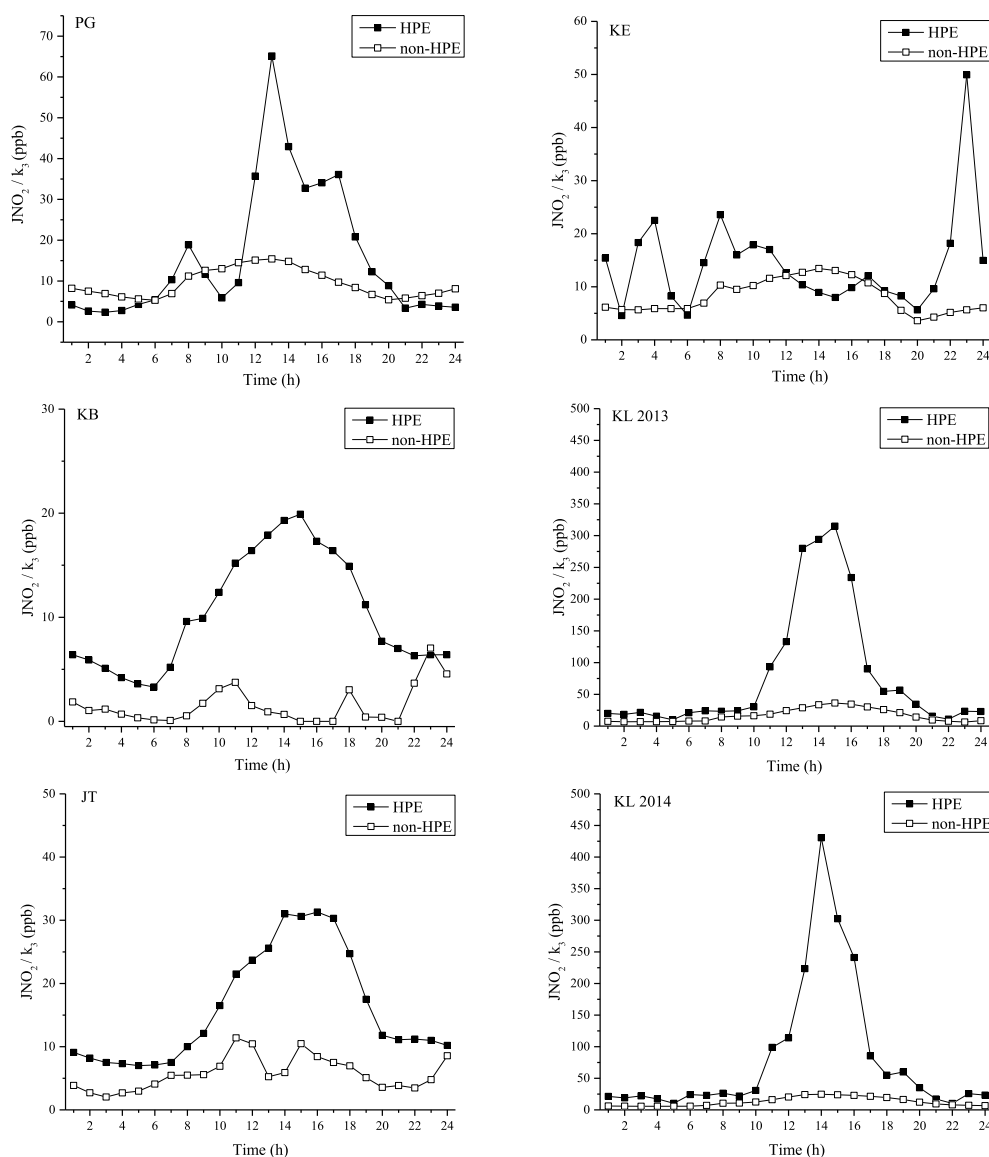


Fig. 4.  $O_3$  photochemistry rate during HPE and non-HPE in 2013 and 2014.

will initiate the photochemical reactions of  $O_3$  formation.

The combination of dry weather and widespread anthropogenic land-clearing fires across Sumatra reduced visibility and air quality across Peninsular Malaysia in June 2013 (Velasco and Rastan, 2015). The decrease in visibility is a direct indicator of an increment in ambient particulate concentrations due to the absorption and scattering of light by gases and particles. Seinfeld and Pandis (2006) elucidated that light scattering by particles is the most important phenomenon that impairs visibility, which is experienced by people living in HPE-affected areas. Malik and Singh (2015) linked atmospheric attenuation to HPE conditions. Atmospheric attenuation is a condition in which sunlight is attenuated by suspended materials in the atmosphere. During HPE, this condition becomes intermittently dominant, particularly in the morning when water droplets are abundant.

Light scattering and atmospheric attenuation are proven to be associated with HPE, which possibly affects  $O_3$  photochemical reactions during HPE periods (Awang et al., 2018).  $O_3$  fluctuations altered CCP time during such periods as depicted in the composite diurnal plots (Fig. 2). Consequently, the CCP occurrence time that is determined using composite diurnal plots also varies, as shown in Table 2. The result suggests that the CCP time for all the stations is 15 min–40 min earlier during HPE. By contrast, the CCP time in PG during HPE (10:50

a.m.) is approximately 20 min delayed compared with that during non-HPE (10:30 a.m.). The DoE (2013) reported that the southern region of Peninsular Malaysia was the most affected area during the 2013HPE, where the maximum diurnal  $PM_{10}$  concentrations in PG reached  $468.75 \mu\text{g}/\text{m}^3$ , which was recorded in June 2013 (Fig. 3). In addition, KL was heavily affected by the event, with the maximum recorded  $PM_{10}$  concentration reaching  $692.75 \mu\text{g}/\text{m}^3$ , whereas the maximum diurnal  $PM_{10}$  concentrations in other stations ranged from  $263.00 \mu\text{g}/\text{m}^3$  to  $406.00 \mu\text{g}/\text{m}^3$ .

A unimodal  $O_3$  peak was observed in all the sites, with maximum concentrations recorded between 12 p.m. and 3 p.m. Meanwhile, the minimum values of  $O_3$  concentrations were recorded at nighttime and early morning hours (near sunrise). The lowest concentrations were consistently measured at 8 a.m. This scenario is probably influenced by NO titration. During morning rush hours, which normally occur from 6 a.m. to 9 a.m., high concentrations of NOx, which comprises  $NO_2$  and NO ‘freshly’ emitted from vehicles and industrial activities (Jiménez-Hornero et al., 2010), and increased NO titration rates in ambient atmosphere reduce  $O_3$  concentrations. NO titration is the most significant sink reaction towards  $O_3$  (Ghazali et al., 2010; Banan et al., 2013; Alghamdi et al., 2014; Latif et al., 2018).

The effective conversion of precursors to  $O_3$  concentration is clearly



**Table 3**  
Pearson correlation of air pollutants during HPE and non-HPE.

Station	Parameter	HPE				non-HPE			
		O <sub>3</sub>	PM <sub>10</sub>	NO <sub>2</sub>	NO	O <sub>3</sub>	PM <sub>10</sub>	NO <sub>2</sub>	NO
PG	O <sub>3</sub> (ppb)	1				1			
	PM <sub>10</sub> (µg/m <sup>3</sup> )	<b>-0.84</b>	1			<b>-0.71</b>	1		
	NO <sub>2</sub> (ppb)	0.31	-0.10	1		-0.53	<b>0.86</b>	1	
	NO (ppb)	<b>-0.69</b>	<b>0.52</b>	<b>-0.38</b>	1	<b>-0.67</b>	<b>0.71</b>	<b>0.39</b>	1
KE	O <sub>3</sub> (ppb)	1				1			
	PM <sub>10</sub> (µg/m <sup>3</sup> )	<b>0.52</b>	1			<b>0.73</b>	1		
	NO <sub>2</sub> (ppb)	<b>0.59</b>	<b>0.52</b>	1		<b>0.48</b>	<b>0.62</b>	1	
	NO (ppb)	<b>-0.65</b>	-0.16	<b>-0.47</b>	1	<b>-0.64</b>	<b>-0.58</b>	-0.31	1
KB	O <sub>3</sub> (ppb)	1				1			
	PM <sub>10</sub> (µg/m <sup>3</sup> )	<b>-0.57</b>	1			<b>-0.66</b>	1		
	NO <sub>2</sub> (ppb)	0.05	<b>0.39</b>	1		<b>-0.76</b>	<b>0.80</b>	1	
	NO (ppb)	<b>-0.53</b>	<b>0.89</b>	0.25	1	<b>-0.60</b>	0.54	<b>0.88</b>	1
KL 2013	O <sub>3</sub> (ppb)	1				1			
	PM <sub>10</sub> (µg/m <sup>3</sup> )	<b>-0.87</b>	1			<b>-0.87</b>	1		
	NO <sub>2</sub> (ppb)	<b>-0.78</b>	<b>0.50</b>	1		<b>-0.77</b>	<b>0.74</b>	1	
	NO (ppb)	<b>-0.81</b>	<b>0.58</b>	<b>0.56</b>	1	<b>-0.80</b>	<b>0.82</b>	<b>0.67</b>	1
JT	O <sub>3</sub> (ppb)	1				1			
	PM <sub>10</sub> (µg/m <sup>3</sup> )	<b>0.60</b>	1			-0.50	1		
	NO <sub>2</sub> (ppb)	<b>0.64</b>	0.44	1		<b>-0.23</b>	<b>0.75</b>	1	
	NO (ppb)	<b>-0.81</b>	<b>-0.73</b>	<b>-0.65</b>	1	0.50	-0.10	0.31	1
KL 2014	O <sub>3</sub> (ppb)	1				1			
	PM <sub>10</sub> (µg/m <sup>3</sup> )	<b>-0.87</b>	1			<b>-0.85</b>	1		
	NO <sub>2</sub> (ppb)	<b>-0.83</b>	<b>0.71</b>	1		<b>-0.79</b>	<b>0.59</b>	1	
	NO (ppb)	<b>-0.79</b>	<b>0.48</b>	<b>0.64</b>	1	<b>-0.81</b>	<b>0.64</b>	0.67	1

\*Bold with significant value at  $p < 0.05$ .

illustrated in the diurnal plot, and the rate of O<sub>3</sub> photochemistry ( $JNO_2/k_3$ ) in PG, KE, KB, KL 2013, KL 2014 and JT are depicted in Fig. 4. The  $JNO_2/k_3$  value fluctuated more during HPE than during non-HPE because the concentrations of O<sub>3</sub>, NO<sub>2</sub> and NO varied daily in all the sites. These results differ from the O<sub>3</sub> daily variations during non-HPE determined by Awang et al. (2016). Theoretically, the  $JNO_2/k_3$  value should be zero during nighttime due to the absence of photochemical reactions (Han et al., 2011). However, the minimum background O<sub>3</sub> concentration in all the sites caused the  $JNO_2/k_3$  value to remain minimal at approximately 3–10 ppb during HPE. The maximum  $JNO_2/k_3$  value occurred in KL 2014 at 2 p.m., reaching 430 ppb during HPE compared with that during non-HPE. Pugliese et al., 2014 and JT recorded the maximum values of 64, 50, 22, 340 and 32 ppb, respectively.

The obtained result showed that the light scattering effect failed to stop O<sub>3</sub> photochemical reactions during HPE. Seinfeld and Pandis (2006) asserted that particle orientation and size are the determinant factors in light scattering intensity, called the unscattered fraction ( $\beta$ ), in the upper hemisphere. At a certain angle, dust particles are completely unscattered with incoming light intensity. At other angles, light is either partially or completely scattered. Despite visibility reduction during HPE, the dust orientation factor caused by a consistent solar intensity reached ground level and maintained a suitable condition for O<sub>3</sub> photochemical reactions, even during HPE.

To further understand the result, the correlation of O<sub>3</sub>, PM<sub>10</sub>, NO<sub>2</sub> and NO observed in all the sites are presented in Table 3. The correlations of O<sub>3</sub> with PM<sub>10</sub> during HPE were positive in KE (0.52) and JT (0.60). Meanwhile, a negative correlation was found in PG, KB, KL 2013 and KL 2014 with -0.84, -0.57, -0.87 and -0.87, respectively. All the results were significant at  $p < 0.05$ . During non-HPE, the correlations of PM<sub>10</sub> with O<sub>3</sub> were negative in all the study areas, except for KE, with 0.73. In summary, a strong negative correlation between O<sub>3</sub> and PM<sub>10</sub> was observed during HPE in KL 2013 and KL 2014, with -0.87. Thus, O<sub>3</sub> concentration during HPE significantly depends on precursor concentrations because an increment in precursors will promote high production in O<sub>3</sub> concentration. The unfavourable trends of O<sub>3</sub> during HPE can possibly lead to increased health risks that require immediate mitigation and prevention plans.

#### 4. Conclusions

This research focused on investigating the influence of PM on the photochemical formation of O<sub>3</sub> during HPE. The influence was investigated during a specific period, known as CCT, which was determined by composite diurnal plots. A comparison was made with non-HPE when PM concentrations were generally low. The result clearly indicates that O<sub>3</sub> concentrations were significantly higher during HPE than during non-HPE in all the sites, but the magnitudes of variation during HPE and non-HPE differed. Changes in CCP time shifted by approximately half an hour later (15–30 min) from non-HPE to HPE. The shift was believed to be caused by the screening effect of PM on morning sunlight. O<sub>3</sub> photochemical formation showed that the  $JNO_2/k_3$  value fluctuated during HPE compared with that during non-HPE as the concentrations of O<sub>3</sub>, NO<sub>2</sub> and NO also varied daily in all the sites. The obtained result showed that the light scattering effect failed to stop O<sub>3</sub> photochemical reactions during HPE. A strong negative correlation between O<sub>3</sub> and PM<sub>10</sub> was observed during HPE in KL 2013 and KL 2014, with -0.87. Therefore, HPE exhibits the tendency to alter the time of O<sub>3</sub> CCP formation.

#### Acknowledgements

This study was funded under the research university individual grant (1001/PAWAM/814278). The authors would like to express their gratitude to Universiti Sains Malaysia and the Department of Environment, Malaysia.

#### References

- Ahmed, M., Guo, X., Zhao, X.M., 2016. Determination and analysis of trace metals and surfactant in air particulate matter during biomass burning haze episode in Malaysia. *Atmos. Environ.* 141, 219–229.
- Ainsworth, E.A., Yendrek, C.R., Sitch, S., Collins, W.J., Emberson, L.D., 2012. The effects of tropospheric ozone on net primary productivity and implications for climate change. *Annu. Rev. Plant Biol.* 63, 637–661.
- Alghamdi, M., Khoder, M., Harrison, R.M., Hyvärinen, A.P., Hussein, T., Al-Jeelani, H., Almeahmadi, F., 2014. Temporal variations of O<sub>3</sub> and NO<sub>2</sub> in the urban background atmosphere of the coastal city Jeddah, Saudi Arabia. *Atmos. Environ.* 94, 205–214.
- Awang, N.R., Ramli, N.A., Yahaya, A.S., Elbayoumi, M., 2015. Multivariate methods to

- predict ground level ozone during daytime, nighttime, and critical conversion time in urban areas. *Atmos. Poll. Res.* 6 (5), 726–734.
- Awang, N.R., Elbayoumi, M., Ramli, N.A., Yahaya, A.S., 2016. The influence of spatial variability of critical conversion point (CCP) in production of ground level ozone in the context of tropical climate. *Aerosol Air Qual. Res.* 16, 153–165.
- Awang, N.R., Ramli, N.A., Shith, S., Zainordin, N.S., Manogaran, H., 2018. Transformational characteristics of ground level ozone during high particulate events in urban areas of Malaysia. *Air Qual. Atmos. Health*. <http://dx.doi.org/10.1007/s11869-018-0578-0>.
- Azmi, S.Z., Latif, M.T., Ismail, A.S., Juneng, L., Jemain, A.A., 2010. Trend and status of air quality at three different monitoring stations in the Klang Valley, Malaysia. *Air Qual. Atmos. Health* 3, 53–64.
- Banan, N., Latif, M.T., Juneng, L., Ahamad, F., 2013. Characteristics of surface ozone concentrations at stations with different backgrounds in the Malaysian Peninsula. *Aerosol Air Qual. Res.* 13 (3), 1090–1106.
- Bergin, M.H., Greenwald, R., Xu, J., Berta, Y., Chameides, W.L., 2001. Influence of aerosol dry deposition on photosynthetically active radiation available to plants: a case study in the Yangtze delta region of China. *Geophys. Res. Lett.* 28 (18), 3605–3608.
- Brimblecombe, P., 2009. Transformation in understanding the health impacts of air pollutants in the 20<sup>th</sup> century. In: Paper Presented at the EPJ Web of Conferences.
- Chattopadhyay, S., Chattopadhyay, G., 2011. Modelling and prediction of monthly total ozone concentrations by use of an artificial neural network based on principal component analysis. *Pure Appl. Geophys.* 1–18.
- Clapp, L.J., Jenkin, M.E., 2001. Analysis of the relationship between ambient levels of O<sub>3</sub>, NO<sub>2</sub> and NO as a function of NO<sub>x</sub> in the UK. *Atmos. Environ.* 35, 6391–6405.
- DoE, 2010. Department of environment, Malaysia. Malaysia environmental quality report 2010. In: M. O. S. Department of Environment, Technology and the Environment, Malaysia.
- DoE, 2013. Department of environment, Malaysia. Malaysia environmental quality report 2013. In: M. O. S. Department of Environment, Technology and the Environment, Malaysia.
- Dominick, D., Latif, M.T., Juahir, H., Aris, A.Z., Zain, S.M., 2012. An assessment of influence of meteorological factors on PM<sub>10</sub> and NO<sub>2</sub> at selected stations in Malaysia. *Sust. Environ. Res.* 22 (5), 305–315.
- Fujii, Y., Tohno, S., Amil, N., Latif, M.T., Oda, M., Matsumoto, J., Mizohata, A., 2015. Annual variations of carbonaceous PM<sub>2.5</sub> in Malaysia: influence by Indonesian peatland fires. *Atmos. Chem. Phys.* 15 (23), 13319–13329.
- Ghazali, N.A., Ramli, N.A., Yahaya, A.S., Md Yusof, N.F.F., Sansuddin, N., Al Madhoun, W., 2010. Transformation of nitrogen dioxide into ozone and prediction of ozone concentrations using multiple linear regression techniques. *Environ. Monit. Assess.* 165 (1), 475–489.
- Han, S., Bian, H., Feng, Y., Liu, A., Li, X., Zeng, F., Zhang, X., 2011. Analysis of the relationship between O<sub>3</sub>, no and NO<sub>2</sub> in tianjin China. *Aerosol Air Qual. Res.* 11, 128–139.
- Hassan, I.A., Basahi, J.M., Ismail, I.M., Habeebullah, T.M., 2013. Spatial distribution and temporal variation in ambient ozone and its associated NO<sub>x</sub> in the atmosphere of Jeddah City, Saudi Arabia. *Aerosol Air Qual Res.* 13, 1712–1722.
- Jiménez-Hornero, F.J., Jiménez-Hornero, J.E., De Ravé, E.G., Pavón-Domínguez, P., 2010. Exploring the relationship between nitrogen dioxide and ground-level ozone by applying the joint multifractal analysis. *Environ. Monit. Assess.* 167 (1–4), 675–684.
- Jones, B.M., Kirby, R., 2009. Quantifying the performance of a top-down natural ventilation Windcatcher™. *Build. Environ.* 44 (9), 1925–1934.
- Latif, M.T., Dominick, D., Ahamad, F., Khan, M.F., Juneng, L., Hamzah, F.M., Nadzir, M.S.M., 2014. Long term assessment of air quality from a background station on the Malaysian Peninsula. *Sci. Total Environ.* 482, 336–348.
- Latif, M.T., Othman, M., Idris, N., Juneng, L., Abdullah, A.M., Hamzah, W.P., Khan, M.F., Sulaiman, N.M.N., Jewaratnam, J., Aghamohammadi, N., Sahani, M., 2018. Impact of regional haze towards air quality in Malaysia: a review. *Atmos. Environ.* <http://dx.doi.org/10.1016/j.atmosenv.2018.01.002>.
- Maghami, M., Hizam, H., Gomes, C., Hajighorbani, S., Rezaei, N., 2015. Evaluation of the 2013 Southeast asian haze on solar generation performance. *PLoS One* 10 (8), 1–19.
- Malik, A., Singh, P., 2015. Comparative analysis of point to point FSO system under clear and haze weather conditions. *Wireless Pers. Commun.* 80 (2), 483–492.
- Md Yusof, N.F., Ramli, N.A., Yahaya, A.S., Sansuddin, N., Ghazali, N.A., Al Madhoun, W., 2010. Monsoonal differences and probability distribution of PM<sub>10</sub> concentration. *Environ. Monit. Assess.* 163 (1), 655–667.
- Mohammed, N.I., Ramli, N.A., Yahya, A.S., 2013. Ozone phytotoxicity evaluation and prediction of crops production in tropical regions. *Atmos. Environ.* 68, 343–349.
- Olmo, N.R.S., Saldiva, P.H.D.N., Braga, A.L.F., Lin, C.A., Santos, U.D.P., Pereira, L.A.A., 2011. A review of low-level air pollution and adverse effects on human health: implications for epidemiological studies and public policy. *Clinics* 66 (4), 681–690.
- Othman, J., Sahani, M., Mahmud, M., Sheikh Ahmad, M.K., 2014. Transboundary smoke haze pollution in Malaysia: inpatient health impacts and economic valuation. *Environ. Pol.* 189, 194–201.
- Ozbay, B., Keskin, G.A., Doğruparmak, Ş.Ç., Ayberk, S., 2011. Multivariate methods for ground level ozone modeling. *Atmos. Res.* 102 (1), 57–65.
- Pugliese, S.C., Murphy, J.G., Geddes, J.A., Wang, J.M., 2014. The impacts of precursor reduction and meteorology on ground-level ozone in the Greater Toronto Area. *Atmos. Chem. Phys.* 14, 8197–8207.
- Rahman, H.A., 2013. Haze phenomenon in Malaysia: domestic or transboundary factor? In: Paper Presented at the 3<sup>rd</sup> International Journal Conference on Chemical Engineering and its Applications (ICCEA'13), Phuket (Thailand), pp. 597–599.
- Reddington, C.L., Yoshioka, M., Balasubramanian, R., Ridley, D., Toh, Y.Y., Arnold, S.R., Spracklen, D.V., 2014. Contribution of vegetation and peat fires to particulate air pollution in Southeast Asia. *Environ. Res. Lett.* 9 (9), 1–12.
- Reid, J.S., Hyer, E.J., Johnson, R.S., Holben, B.N., Yokelson, R.J., Zhang, J., Campbell, J.R., Christopher, S.A., Di Girolamo, L., Giglio, L., Holz, R.E., 2013. Observing and understanding the Southeast Asian aerosol system by remote sensing: an initial review and analysis for the Seven Southeast Asian Studies (7SEAS) program. *Atmos. Res.* 122, 403–468.
- Seinfeld, J.H., Pandis, S.N., 2006. *Atmospheric Chemistry and Physics*, second ed. John Wiley: A Wiley-Interscience Publication Press.
- Sousa, S., Martins, F., Alvim-Ferraz, M., Pereira, M., 2007. Multiple linear regression and artificial neural networks based on principal components to predict ozone concentrations. *Environ. Model. Software* 22 (1), 97–103.
- Toh, Y.Y., Lim, S.F., Von Glasow, R., 2013. The influence of meteorological factors and biomass burning on surface ozone concentrations at Tanah Rata, Malaysia. *Atmos. Environ.* 70, 435–446.
- Turias, I.J., González, F.J., Martín, M.L., Galindo, P.L., 2008. Prediction models of CO, SPM and SO<sub>2</sub> concentrations in the Campo de Gibraltar Region, Spain: a multiple comparison strategy. *Environ. Monit. Assess.* 143 (1–3), 131–146.
- Velasco, E., Rastan, S., 2015. Air quality in Singapore during the 2013 smoke-haze episode over the Strait of Malacca: lessons learned. *Sustain. Cities Society* 17, 122–131.
- Wang, Z.H., 2003. The research on the aerosol dust deposition monitoring. *J. Arid Land Resour. Environ.* 17 (1), 54–59.
- Xu, J., Tai, X., Betha, R., He, J., Balasubramanian, R., 2015. Comparison of physical and chemical properties of ambient aerosols during the 2009 haze and non-haze periods in Southeast Asia. *Environ. Geochem. Health* 37 (5), 831–841.
- Zhou, J., Chen, A., Cao, Q., Yang, B., Chang, V.W.C., 2015. Particle exposure during the 2013 haze in Singapore: importance of the built environment. *Built. Environ.* 93, 14–23.